How to Cite: Shahid, Z.A., & Tabassum, R. (2025). Mn(II) and Zn(II) Complexes of a Coumarin Derivative: Synthesis, Characterization and Biological Potential. *Eurasian Journal of Chemistry.* https://doi.org/10.31489/2959-0663/4-25-11

Article

Received: 18 August 2025 | Revised: 27 November 2025 |
Accepted: 4 December 2025 | Published online: 12 December 2025

UDC 546.65; 547.442

https://doi.org/10.31489/2959-0663/4-25-11

Zulfiqar Ali Shahid, Rukhsana Tabassum*

Institute of Chemistry, Islamia University of Bahawalpur, Bahawalpur, Pakistan
*(*Corresponding author's e-mail: rukhsana.tabassum@iub.edu.pk)*

Mn(II) and Zn(II) Complexes of a Coumarin Derivative: Synthesis, Characterization and Biological Potential

This study focused on the synthesis, characterization and biological evaluation of coumarin derivatives and their metal complexes. The synthesized compounds were characterized using spectroscopic techniques, including FTIR, ^{1}H NMR, ^{13}C NMR, X-ray diffraction (XRD), and thermal analysis, with mass spectrometry confirming their molecular weights. Notably, the XRD analysis revealed crystal sizes of 4.092 nm for ZL16, 4.34 nm for ZL16Mn, and 1.57 nm for ZL16Zn. FTIR analysis confirmed the presence of the –N=N– group, and comparative UV-Visible spectra validated the successful synthesis of new coumarin compounds. Antibacterial activity of synthesized compounds was evaluated against gram-negative and gram-positive bacteria using the disc diffusion method, with inhibition zones ranging from 7–31 mm, compared to the standard drug Amikacin, which had a zone of 15 mm. Antioxidant activity was assessed with IC_{50} values between 5.65–11.84 µg/mL for DPPH and 5.89–11.20 µg/mL for NO, compared to ascorbic acid. Molecular Docking analysis revealed strong binding interactions between the synthesized compounds and the Mannosyl-oligosaccharide glucosidase and Oligo-1,6-glucosidase enzymes, with binding energies ranging from –9.8 to –10.9 kcal/mol. These findings contribute to the field of medicinal chemistry, highlighting the potential of these compounds as therapeutic agents. Further investigations are required at molecular level to explore their full therapeutic potential.

Keywords: coumarin derivatives, manganese, zinc metal complexes, antioxidant activity, antibacterial activity, molecular docking, X-ray diffraction, thermal analysis, antidiabetic

Introduction

The term *coumarins* comes from the French word *coumarou*, meaning "tonka bean." The study of coumarin began in 1820 when Vogel first extracted it from tonka beans [1]. Coumarins are basically known for its vanilla-like or freshly-mowed hay-like fragrance. It is white crystalline powder with a sweet aromatic odour with certain nutty shadings [2]. Coumarin derivatives are gaining significant attention in the field of medicine due to their physiological activity [3]. These compounds have shown promising potential in metal-based drug chemistry for the treatment of sensitive cancers [4]. Coumarin, a type of heterocyclic organic compound, is widely utilized in analytical and biological fields [5]. It contains a benzopyrone ring with an oxygen functional group, making it an effective donor, It also have a wide range of applications, including being used as anticoagulants, spasmolytic, anticancer drugs, antibacterial, antithrombotic, vasodilatory, antioxidant effects, and plant growth regulators as given in Figure 1 [6]. Based on these findings, a Schiff base ligand containing coumarin moieties was synthesized, along with its metal complexes, and their antimicrobial and antioxidant activities were studied [7]. Metal complexes of coumarins have been extensively studied for their medicinal applications and have shown greater biological activity compared to their ligands [8]. The chelating ability of coumarin derivatives, enhances their biological activity [9]. Additionally, synthetic coumarins have found applications as fluorescent brightening agents [10]. In a specific study, bivalent metal complexes of a coumarin derivatives were synthesized and evaluated spectroscopically and biologically [11]. Schiff bases, another class of ligands, have interesting coordination modes towards various metals and have been studied for their biological applications [12]. Coumarin derivatives, particularly hydroxycoumarins, exhibit antioxidant properties and metal chelating abilities [13]. The antioxidant activity of metal complexes is influenced by both the metal and the ligands [14].

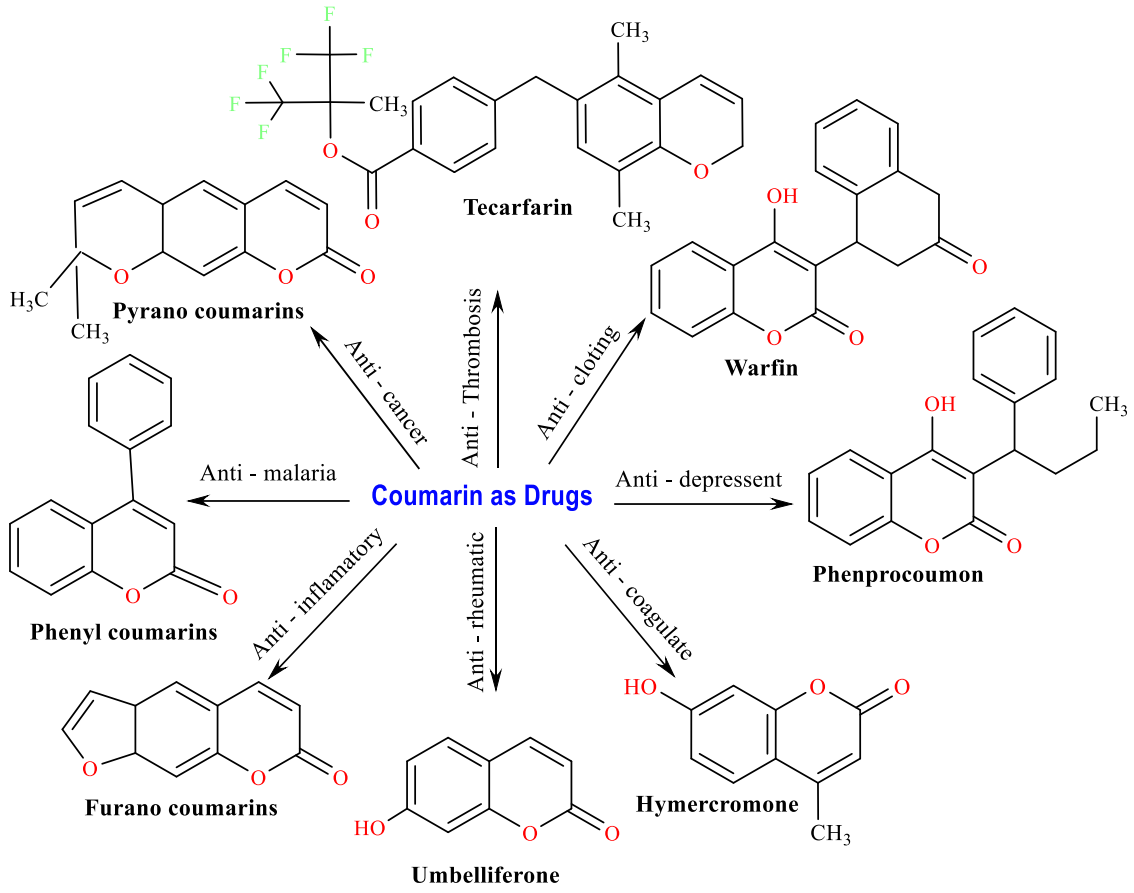

Figure 1 Some commercially available coumarin derivatives

Overall, the research discussed highlights the importance of heterocyclic compounds with nitrogen atoms, specifically coumarin derivatives, in various medicinal applications [15]. The synthesis and evaluation of metal complexes and the exploration of their biological activities contribute to the understanding of their potential in drug development and disease treatment [16]. In this paper we are reported an efficient route for the synthesis of new Mn(II), and Zn(II) complexes obtained from (4-Hydroxy coumarin) coumarin [17]. The thermal decomposition of their complexes is also used to infer the structure and the different thermodynamic activation parameters are calculated [18]. Synthetic coumarins have been used as fluorescent brightening agents in textiles, paper, detergents and dyes [19].

Furthermore, the aim for studying the interaction between synthesized ligands and α-glucosidase using molecular docking is to explore alternative strategies for managing type 2 diabetes (T2DM). α-Glucosidase inhibitors (AGIs), such as acarbose, are effective in controlling postprandial blood glucose levels but come with gastrointestinal side effects. First-row transition metal complexes, particularly those involving zinc and other metals, have shown promise as α-glucosidase inhibitors, potentially offering advantages like lower toxicity and novel mechanisms of action [20]. Molecular docking studies help predict the binding affinities and interaction modes of these complexes with the enzyme, aiding in the design of more effective inhibitors. This approach aims to overcome the limitations of traditional AGIs, offering a promising alternative for T2DM treatment with potentially fewer side effects and improved efficacy.

Experimental

Chemicals and Solvents

All chemicals like 4-hydroxycoumarin, 2-aminophenol, 2-amino-5-chlorobenzophenone, o-toluidine, 2'-amino-2,5-dichlorobenzophenone, 2-chloroaniline, p-toluidine, sodium nitrite ($NaNO_2$), HCl, NaOH (base) and solvents; ethanol, methanol, distilled water, dimethylsulfoxide (DMSO), tetrahydrofuran (THF), carbon tetrachloride (CCl_4), acetone, benzene, n-hexane, chloroform, dimethylformamide (DMF) were purchased from sigma Aldrich, Merck, Alfa Aesar and BDH and were used without further purification.

Instruments

Silica gel plates were used to monitor the progress of reaction by thin layer chromatography technique which were visualized under UV. Melting points were recorded by open capillary method on Stuart SMP10 and are uncorrected. The FTIR spectra were obtained using a BRUKER Tensor 27 (M15E-PS/09) FTIR spectrophotometer, using KBr discs. The spectral range was covered from 4000 to 400 cm^{-1}. The ^{13}C NMR and ^{1}H NMR spectra were acquired using a Bruker-300 MHz spectrometer. The DPPH and NO scavenging activity were assessed using an Optima SP300-spectrophotometer. UV-visible spectra were recorded using ELISA reader. Powdered XRD data was obtained using BRUKER D8 X-ray diffractometer. The molecular mass of compounds was measured using JEOL 600H-1mass spectrometer. TGA analysis was recorded on a Shimadzu TGA-50H.

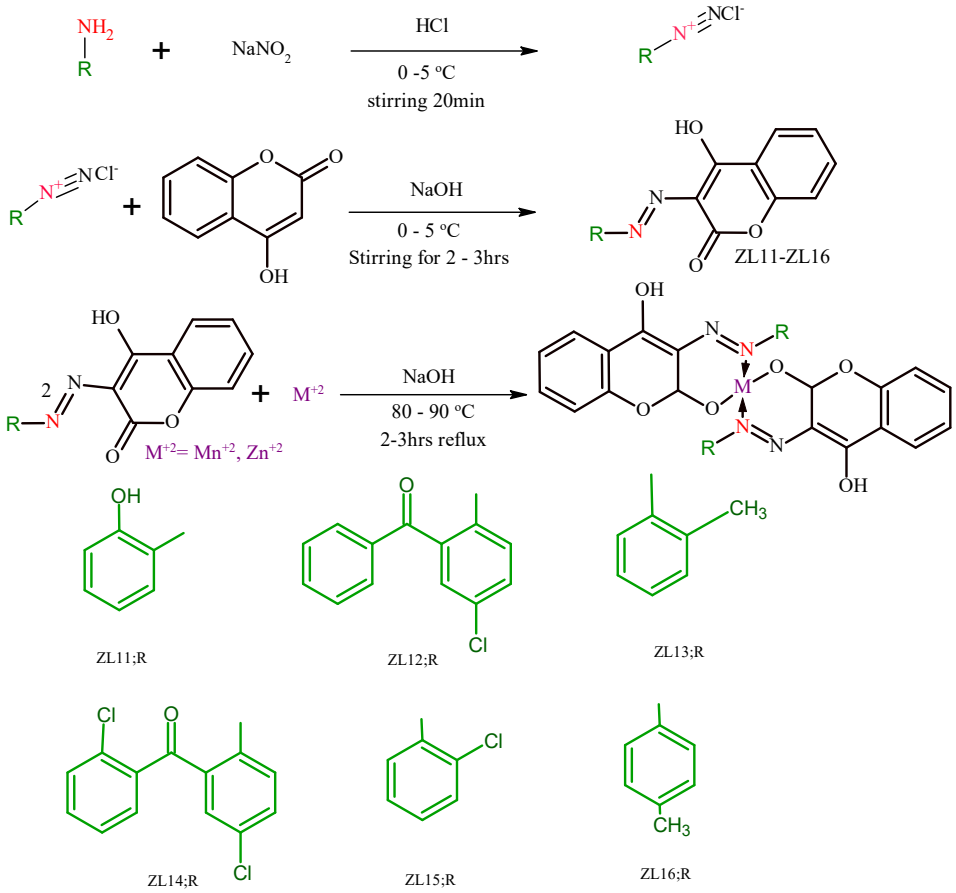

Scheme 1. Synthetic route for coumarin derivatives and their metal complexes

Preparation of Ligands

General Procedure for the Synthesis of Coumarin Derivatives ZL11-ZL16

A 10 mL solution of 3 M hydrochloric acid (HCl) was prepared and combined with a substituted aniline compound. Gradually, an aqueous solution of sodium nitrite ($NaNO_2$) was added, resulting in the formation of a diazonium salt. Then, a solution of 4-hydroxycoumarin was introduced to the reaction mixture, which was placed in an ice bath for 20 minutes to maintain the optimal temperature of 0–5 °C. The coupling between the diazonium salt and 4-hydroxycoumarin occurred under these conditions. Neutralization was achieved by adding 3 M sodium hydroxide (NaOH) to the mixture, and the reaction was stirred for 2–3 hours at 0–5 °C, facilitating the formation of the coumarin ligand (ZL). The synthesized product was collected by filtration and purified through recrystallization in ether, yielding up to 87 %. The reaction completion and purity of the compound were assessed using thin-layer chromatography (TLC) analysis (Scheme 1).

Metallization of Metal Complexes of Ligands ZL11-ZL16

To synthesize the Mn^{2+} and Zn^{2+} metal complexes, a 0.5 mmol solution of the coumarin derivative was prepared in ethanol and stirred continuously for 5 minutes. An ethanolic solution of the metal salts (Zn^{2+} or Mn^{2+}) was then added in a 1:2 metal-to-ligand ratio, and the mixture was stirred for 20 minutes. Sodium hydroxide was added dropwise under reflux conditions to adjust the pH to approximately 8, creating a basic environment. A visible color change occurred, indicating the formation of the metal complex (MZL). The reaction was allowed to proceed under reflux at a temperature range of 80–90 °C for 2 hours. The product was collected, washed with distilled water, and dried for further use.

4-hydroxy-3-[(E)-(2-hydroxyphenyl)diazenyl]-2H-chromen-2-one (ZL11). Brown solid, yield: 79.28 %, Rf: 0.56 (acetone:CCl_4 (1:1)), soluble in THF, DMF, DMSO, acetone, ethanol, methanol, chloroform, n-hexane, and benzene m.p.: 182 °C, FTIR (KBr disc, cm^{-1}): 3080.72 (NH stretch, O–H stretch), 1741.87 (C=O), 1610.11 (N=N stretch), 1645.43 (C=C stretch), 1525.03 (C–C stretch), 1346.60 (C–N stretch), 1190.63 (C–O stretch), UV-Visible, λ_{max} (DMSO, nm): 590, ^{1}H NMR (300 MHz, DMSO-D6) δ 15.9 (s, OH), 8.03 (D, J = 7.8 Hz, Hd), 7.92 (s, Hb, Hg), 7.79 (s, Hc), 7.66 (s, He), 7.56 (s, Ha), 5.59 (s, Hh). ^{13}C NMR (100 MHz, DMSO) δ 178.5 (C4), 163.7 (C2), 154.1 (C6), 151.9 (C14), 137.2 (C17), 130.1 (C15, C16), 129.1 (C19), 128.7 (C18), 124.7(C9), 124.0 (C10), 117.7 (C7), 116.7 (C5), 102.3 (C3), 19.3 (C21). EI-MS m/z: Required for $C_{15}H_{10}N_2O_4^{+}\cdot$: 282.25 found 282.2.

3-[(E)-(2-benzoyl-4-chlorophenyl)diazenyl]-4-hydroxy-2H-chromen-2-one (ZL12). Yellowish Orange solid, yield: 79.81 %, Rf: 0.72 (CCl_4:chloroform (2:8)), soluble in THF, DMF, DMSO, acetone, ethanol, methanol, chloroform, n-hexane, and benzene m.p: 290 °C, FTIR (KBr disc, cm^{-1}): 3008.02 (NH stretch, O–H stretch), 1738.65 (C=O), 1625.81 (N=N stretch), 1661.61 (C=C stretch), 1396.68 (C–C stretch), 1290.64 (C–N stretch), 1067.10 (C–O stretch) UV-Visible, λ_{max} (DMSO, nm):380, ^{1}H NMR (300 MHz, DMSO-D6) δ 7.77–7.68 (m, He), 7.59 (d, J = 6.5 Hz, Hg), 7.54 (d, J = 5.5 Hz, Hk, Hi), 7.52 (s, Ha, Hc), 7.48–7.38 (m, Hb, Hj), 7.32 (s, Hi, Hh), 7.12 (s, Hf), 6.88 (s, Hh, Hd). ^{13}C NMR (100 MHz, DMSO) δ 196.7 (C21), 150.5 (C4), 139.1 (C2), 1133.9 (C24, C6), 132.6 (C27, C18, C15), 131.2 (C17), 128.4 (C29, C25, C16), 120.0 (C7, C5), 116.9 (C3). EI-MS m/z: Required for $C_{22}H_{13}ClN_2O_4^{+}\cdot$: 404.80 found 404.0.

4-hydroxy-3-[(E)-(2-methylphenyl) diazenyl]-2H-chromen-2-on (ZL13). Light Greenish solid, Yield: 89.28 %, Rf: 0.63 (CCl_4:chloroform (2:8)), soluble in THF, DMF, DMSO, acetone, ethanol, methanol, chloroform, n-hexane, and benzene, m.p: 196 °C, FTIR (KBr disc, cm^{-1}): 3350.62 (NH stretch, O–H stretch), 1735.97 (C=O), 1599.37 (N=N stretch), 1544.49 (C=C stretch), 1328.21 (C–N stretch), 1234.68 (C–O stretch) UV-Visible, λ_{max} (DMSO, nm): 660, ^{1}H NMR (300 MHz, DMSO-D6) δ 12.53 (s, OH), 7.82 (d, J = 1.7 Hz, Ha, Hd), 7.80 (d, J = 1.7 Hz, He), 7.53 (s, Hf), 7.33 (d, J = 1.1 Hz, Hb, Hc, Hh), 5.59 (s, Hg), 3.37 (s, CH_3). ^{13}C NMR (100 MHz, DMSO) δ: 177.6 (C4), 166.5 (C2), 162.5 (C6), 154.0 (C15), 151.9 (C16), 136.4 (C8), 132.3 (C17), 131.1 (C19), 130.1 (C9), 123.8 (C5), 102.3 (C7), 90.9 (C3). EI-MS m/z: Required for $C_{16}H_{12}N_2O_3^{+}\cdot$: 280.87 found 280.87.

3-{(E)-[4-chloro-2-(2-chlorobenzoyl) phenyl] diazenyl}-4-hydroxy-2H-chromen-2-one (ZL14). Dark Orange solid, Yield: 79.81 %, Rf: 0.65 (CCl_4:ethanol (3:7)), soluble in THF, DMF, DMSO, acetone, ethanol, methanol, chloroform, n-hexane, and benzene m.p: 226 °C, FTIR (KBr disc, cm^{-1}): 3399.49 (NH stretch, O–H stretch), 1739.99 (C=O), 1596.09 (N=N stretch), 1465.96 (C=C stretch), 1403.68 (C–N stretch), 712.75 (C–Cl stretch), 1067.88 (C–O stretch) UV-Visible, λ_{max} (DMSO, nm): 660, ^{1}H NMR (300 MHz, DMSO-D6) δ: 16.36 (s, OH), 7.84–7.78 (m, He), 7.66 (s, Hb, Hj), 7.58 (d, J = 7.9 Hz, Ha, Hc, Hg), 7.58–7.52 (m, Hi, Hk), 7.49–7.46 (m, Hh, Hf), 7.43 (d, J = 7.4 Hz, Hh). ^{13}C NMR (100 MHz, DMSO) δ: 194.9 (C21), 164.4 (C4), 138.3 (C2), 133.9 (C25, C15), 132.6 (C27, C17, C24), 131.2 (C8, C16), 128.4 (C29, C18), 120.0 (C9, C10), 117.1 (C5) 116.1 (C7), 90.9 (C3). EI-MS m/z: Required for $C_{22}H_{12}Cl_2N_2O_4^{+}$: 439.24 found 439.3.

3-[(E)-(2-chlorophenyl) diazenyl]-4-hydroxy-2H-chromen-2-one (ZL15). Brown solid, Yield: 83.33 %, Rf: 0.63 (CCl_4:benzene (3:7)), soluble in THF, DMF, DMSO, acetone, ethanol, methanol, chloroform, n-hexane, and benzene m.p: 172 °C, FTIR (KBr disc, cm^{-1}): 3366.65 (NH stretch, O–H stretch), 1739.98 (C=O), 1607.69 (N=N stretch), 1571.03 (C=C stretch), 1394.26 (C–N stretch), 742.93 (C–Cl stretch), 1081.74 (C–O stretch); UV-Visible, λ_{max} (DMSO, nm): 660, ^{1}H NMR (300 MHz, DMSO-D6) δ: 15.98 (s, OH), 8.03 (d, J = 7.8 Hz, He), 7.92 (d, J = 8.3 Hz, Ha, Hd), 7.79 (t, J = 7.7 Hz, Hh), 7.66 (d, J = 7.9 Hz, Hb, Hc), 7.56 (d, J = 7.7 Hz, Hf), 7.37 (d, J = 2.5 Hz, Hg). ^{13}C NMR (100 MHz, DMSO) δ: 165.4 (C4), 161.8 (C2), 153.5 (C6), 132.9 (C15), 123.9 (C19, C17), 116.7 (C5), 116.4 (C7), 91.7 (C3). EI-MS m/z: Required for $C_{15}H_9ClN_2O_3^{+}\cdot$: 300.69 found 300.1.

4-hydroxy-3-[(E)-(4-methylphenyl)diazenyl]-2H-chromen-2-one (ZL16). Light yellow solid, yield: 89.84 %, Rf: 0.73 (methanol:CCl_4 (3:7)), soluble in THF, DMF, DMSO, acetone, ethanol, methanol, chloroform, n-hexane, and benzene, m.p.: 211 °C, FTIR (KBr disc, cm^{-1}): 3352.50 (NH stretch, O–H stretch), 1740.31 (C=O), 1647.46 (N=N stretch), 1543.45 (C=C stretch), 1328.16 (C–N stretch), 1236.66 (C–O stretch), UV-Visible, λ_{max} (DMSO, nm): 620; ^{1}H NMR (300 MHz, DMSO-D6) δ: 15.51 (s, OH), 7.82–7.80 (m, Hd, Ha), 7.65–7.63 (m, He, Hf), 7.36 (d, J = 1.4 Hz, Hb, Hc), 5.58 (s, Hg, Hh), 2.49 (s, Hi, Hj, Hk). ^{13}C NMR (100 MHz, DMSO) δ: 178.5 (C4), 163.7 (C2), 154.1 (C6), 151.9 (C14), 137.2 (C17), 130.1 (C15, C16), 129.1 (C19), 128.7 (C18), 124.7(C9), 124.0 (C10), 117.7(C7), 116.7(C5), 102.3 (C3), 19.3(C21). EI-MS m/z: Required for $C_{16}H_{12}N_2O_3^{+}\cdot$: 280.27 found 280.2

4-hydroxy-3-[(E)-(4-methylphenyl) diazenyl]-2H-chromen-2-one Manganese complex (ZL16Mn). Pale yellow solid, m.p.: >300 °C, yield: 89.53 %, soluble in chloroform, THF, acetone, DMSO, benzene, CCl_4, ethanol, methanol, DMF and n-hexane, FTIR (KBr disc, cm^{-1}): 1632.76 (N=N stretch), 1414.64 (C–N stretch), 1321.97 (C–O stretch), 577.02 (Mn–O), 516.37 (Mn–N), UV-Visible λ_{max} (DMSO, nm): 660.

4-hydroxy-3-[(E)-(4-methylphenyl) diazenyl]-2H-chromen-2-one Zinc complex (ZL16Zn). Dark yellow solid, m.p.: >300 °C, yield: 86.49 %, soluble in acetone, ethanol, methanol DMSO, benzene, CCl_4, chloroform, THF, DMF and n-hexane, FTIR (KBr disc, cm^{-1}): 3391.93 (NH stretch, O–H stretch), 1513.02 (N=N stretch), 1650.25 (C=C stretch), 1561.28 (C–C stretch), 1342.96 (N=O stretch), 1350.20 (C–N stretch), 1058.16 (C–O stretch), 761.28 (C–Cl stretch), 669.83 (Zn–O), 521.04 (Zn–N), UV-Visible λ_{max} (DMSO, nm): 380.

Anti-Oxidant Scavenging Assay

Antioxidant compounds found in food are crucial for maintaining good health and reducing the risk of chronic diseases like heart disease and cancer. These antioxidants are primarily found in fruits, whole grains, and vegetables. Plant-based antioxidants, such as vitamin E, vitamin C, carotenes, phytoestrogens, phytate, and phenolic acids, have been recognized for their potential to lower disease risk. The diverse range of antioxidant compounds in our diet have varying levels of antioxidant activity, with some being strong antioxidants, like gallates, and others being weaker, like mono-phenols. The main function of antioxidants is to neutralize free radicals by donating hydrogen atoms, thereby reducing them to non-reactive species. By removing the odd electron feature responsible for radical reactivity, antioxidants help protects against the harmful effects of free radicals. Free radicals have garnered significant attention from scientists due to their wide-ranging impact on biological systems, including their involvement in disease development and aging. It has been established that oxidative stress, caused by an imbalance between antioxidants and free radicals, contributes to the pathogenesis of certain diseases. Therefore, there is evidence supporting the use of antioxidant supplementation to reduce oxidative stress levels and potentially slow down or prevent disease-related complications. While synthetic antioxidant components have been found to have toxic and mutagenic effects, natural antioxidants have gained attention due to their safer profile [21].

Diphenyl-2-Picrylhydrate (DPPH) Free Radical Scavenging Assay

The antioxidant activity of the synthesized compounds against 2,2-diphenyl-2-picrylhydrate (DPPH) were evaluated [22]. The standard used was ascorbic acid and various concentration (5, 10, 15, 20, and 25 μg/ml) of the compounds were measured using Optima SP300-spectrophotometer at 517 nm [23].

The experiment was triplicates and % scavenging was calculated by using formula.

$$\%\text{Scavenging} = ((\text{Ao} - \text{As}))/\text{Ao}\times 100,$$

where Ao — is the absorbance of blank; As — is the absorbance of sample.

Absorbance of sample was calculated by using formula:

$$\text{As} = \text{Ast} - \text{Asb},$$

where As — is the absorbance of sample; Ast — is the absorbance of test sample solution with DPPH; Asb — is the absorbance of blank sample solution without DPPH.

The IC_{50} value, defined as the concentration of the tested compounds required to scavenge 50 % of DPPH free radicals, was calculated by non-linear regression using GraphPad Prism 8 (GraphPad Software Inc., La Jolla, USA).

Nitric Oxide (NO) Free Radical Scavenging Assay

Sodium nitroprusside was used for nitric oxide production in aqueous solution at 7.4 pH which combine with oxygen to give nitrite ion which one determined by using Griess reagent. For this aim to 2 mL of various concentration (5, 10, 15, 20 and 25 μg/ml) of sample solution in DMSO, 2 mL of 10 mL sodium nitro-

prusside in PBS (phosphate buffer saline) solution was added and incubated at 25 °C for 4 hours. After incubation to 2 mL of reaction solution containing nitrate ion 2 mL of Griess reagent (1 % sulphanilamide in 5 % phosphoric acid (1 mL) and 0.1 % N-(1-naphthyl)ethylenediamine dihydrochloride (1 mL) was added and again incubated at 25 °C for 30 minutes. Same reaction mixture instead test compound having 2 mL DMSO served as blank. The absorbance of chromophore formed was measured at 546 nm using Optima SP300-spectrophotometer. The experiment was done in triplicate and % scavenging was calculated by using formula:

$$\%\text{Scavenging} = ((\text{Ao} - \text{As}))/\text{Ao}\times 100,$$

where Ao — is the absorbance of blank; As — is the absorbance of sample.

Absorbance of sample was calculated by using formula:

$$\text{As} = \text{Ast} - \text{Asb},$$

where As — is the absorbance of sample; Ast — is the absorbance of test sample solution with DPPH; Asb — is the absorbance of blank sample solution without DPPH.

The IC_{50} value, defined as the concentration of the tested compounds required to scavenge 50 % of NO free radicals, was calculated by non-linear regression using GraphPad Prism 8 (GraphPad Software Inc., La Jolla, USA).

Anti-Bacterial Activities

The synthesized compounds were studied for the antibacterial activity against the bacterial species All the synthesized ligands (ZL11-ZL116) and their metal complexes with (Mn(II), Zn(II)) (Figure S1–S18). The Zone of inhibitions of synthesized compounds were carried out by disc diffusion method [24]. The antibacterial activity of all the synthesized ligands was evaluated against 24 hr culture of various selected bacteria. The gram-negative bacteria used were *E. Coli* and *Pseudomonas aeruginosa* while gram-positive bacteria were *Staphylococcus Pyogenes* and *Bacillus*. Amikacin was used as standard drug for the evaluation of antibacterial activity. Activity was reported by zone of inhibition (mm)[25].

Molecular Docking Protocol

In this study, we aimed to investigate the binding interactions between newly synthesized coumarin derivatives and two enzymes, namely Mannosyl-oligosaccharide glucosidase and Oligo-1,6-glucosidase. To initiate, we obtained the 3D crystal structures of these enzymes from the Protein Data Bank (www.rcsb.com) with the Mannosyl-oligosaccharide glucosidase structure having a resolution of 2.04Å (PDB ID: 4J5T) and the Oligo-1,6-glucosidase structure having a resolution of 1.30Å (PDB ID: 3AJ7). Before conducting the docking analysis, we prepared the structures of the target proteins using MGL tools. Heteroatoms and water molecules present in protein structures were removed. Additionally, polar hydrogen atoms and Kollman charges were added to ensure the accurate representation of the protein structures. Furthermore, any missing amino acid residues were rendered in the structures to ensure their structures. Furthermore, we generated the 3D structures of the synthesized coumarin derivatives (ZL11-ZL16) using ChemDraw 3D [26]. These structures were then subjected to energy minimization to obtain their most stable conformations. For the docking analysis, the we utilized AutoDock, employing its default genetic algorithm as the scoring function. The compounds (ZL11-ZL16) were docked into the active pockets of Mannosyl-oligosaccharide glucosidase and Oligo-1,6-glucosidase. The dimensions of gird box were set as *x*: 21.306612; *y*: –0.461484; *z*: 18.843785 for Mannosyl-oligosaccharide glucosidase and *x*: –18.523631; *y*: –20.732132; *z*: 8.202425 for Oligo-1,6-glucosidase to define the search space for docking respectively. Multiple docking configurations were generated for each compound and enzyme, resulting in approximately 100 different configurations. Finally, to attain a deeper insight of the binding interactions occurring within the active sites of Mannosyl-oligosaccharide glucosidase and Oligo-1,6-glucosidase, the most stable configurations were selected for further analysis and development of 2D and 3D models to understand the binding interactions among the derivatives within the active sites of Mannosyl-oligosaccharide glucosidase and Oligo-1,6-glucosidase.

Results and Discussion

Coumarin derivatives were synthesized utilizing a previously documented procedure, resulting in a remarkable yield. The confirmation of these derivatives was accomplished by analyzing their physical spectroscopic parameters. Subsequently, complexes of transition metals (Mn^{+2}, Zn^{+2}) with these Coumarin derivatives were synthesized and subjected to characterization based on various physical properties, including solubility, melting point, as well as spectroscopic techniques such as UV-visible spectroscopy, FTIR spectros-

copy, X-ray diffraction, and Thermal gravimetric analysis. To ensure conformity with existing literature regarding the synthesis of metal complexes, the coordination of ligands with metal ions was investigated. Initially, Job's method was employed to determine the optimal stoichiometric ratio, and it was observed that a 2:1 ratio of ligands to metals yielded the highest absorbance [27]. Consequently, the metal complexes were synthesized utilizing this specific stoichiometric ratio of ligands and metal salts [28]. Regarding the thermal stability of these metal complexes, it was observed that Mn(II) and Zn(II) complexes exhibited melting points exceeding 300 °C, while the coumarin derivatives themselves displayed a melting point range of 150–300 °C. This discrepancy indicates that the metal coordination compounds of the derivatives exhibit significantly enhanced stability due to the smaller size and higher charge of the Mn and Zn complexes [29]. Furthermore, all complexes demonstrated solubility in DMSO.

Spectroscopic Characterization

FTIR Characterization of Synthesized Coumarin Derivatives

FTIR spectra of all synthesized coumarin derivatives were recorded in 400–6000 cm^{-1} region which gave valuable information about formation and structure of all the synthesized coumarin ligand. The FTIR spectra showed prominent peaks of functional groups like O–H, C–H, C=O, C=N, N=N, C=C, C–N and C–O which confirms the formation of coumarin derivatives [30]. The appearance of a broad peak of O–H stretch near 3650–3200 cm^{-1}, N–H stretch appeared around 3600–3400 cm^{-1}. Appearance of a distinctive peak of N=N of diazinyl group at around 1700–1400 cm^{-1} were observed in FTIR spectra of ligands confirmed the presence of these functional groups. The vibrational frequency for sp^2 CH stretch was observed around 3000–2800 cm^{-1} which is region according to literature. Since O–H has a broad peak so it overlapped with aromatic C–H stretch. Another peak C=C stretch was observed near 1520–1400 cm^{-1} and aromatic C–N stretch was seen at 1390–1180 cm^{-1}. While C–O stretch was observed in 1320–900 cm^{-1}, it was seen that all the above-mentioned peaks are in IR region according to literature. For all the metal complexes M–O stretch was shifted towards lower frequency in complexes because nitrogen was involved in complex formation. For exemplary, FTIR spectra of ligand ZL14 (Fig. 2) with its complexes (Zn^{+2}, Mn^{+2}) were discussed for comparative study.

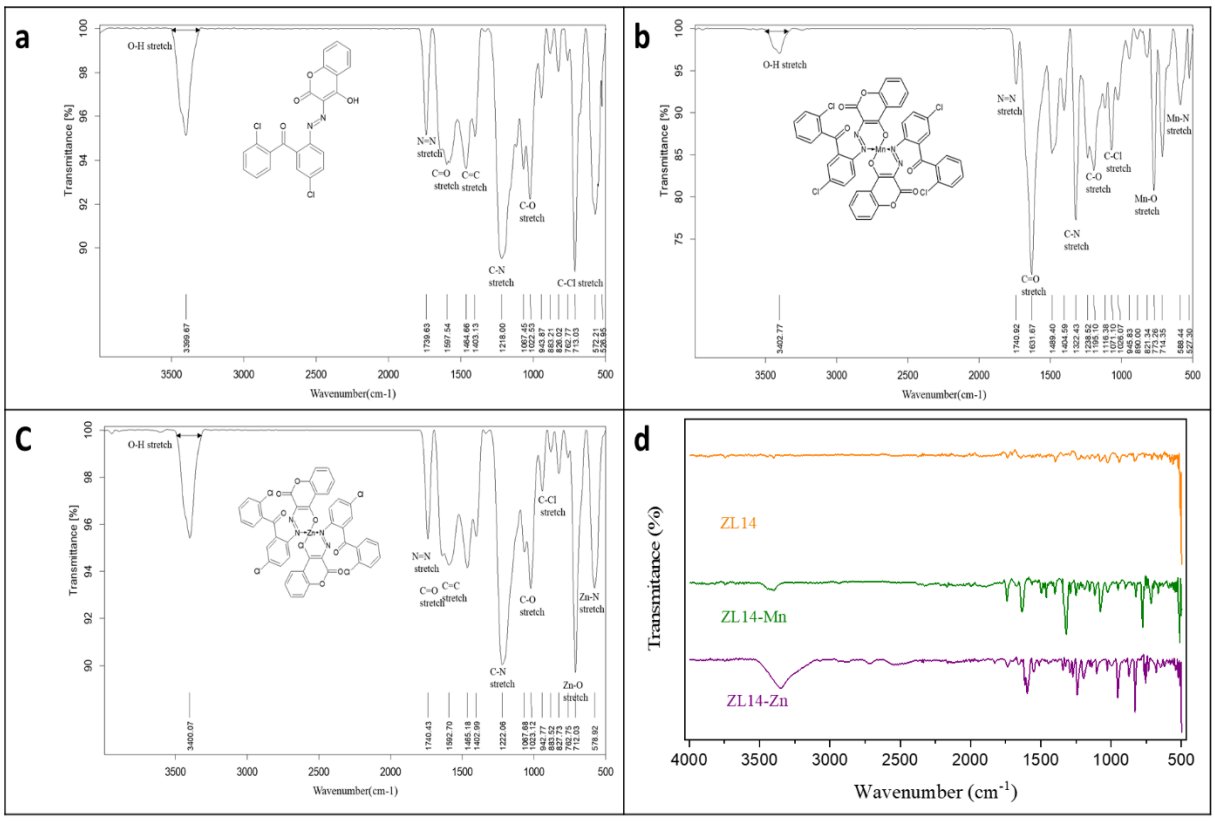

Figure 2. FTIR spectra of (*a*) ZL14 (*b*) ZL14Mn (*c*) ZL14Zn (*d*) comparative FTIR spectra of ZL14 and its transition metal complexes

The stretching frequency for dizenyl group N=N was observed at 1596.09 cm^{-1}, a broad and sharp peak of OH was seen at 3399.49 cm^{-1}. The Aromatic =C–H stretch was observed near 3251.09 cm^{-1}. The vibrational frequency of C=O was observed at 1739.99 cm^{-1}, C–N and C–O stretch were seen at 1403.68 and 1022.88 cm^{-1} respectively while sp^2 C–H stretch were observed near 3251.09 cm^{-1}. The C=O peak appeared near 1739.99 cm^{-1}. M–O stretch for all metal complexes appeared below 591.63 and 712.08 cm^{-1} for Mn(II) and Zn(II) respectively. Similarly, Mn(II) and Zn(II) stretch at 516.99 and 577.64 cm^{-1} respectively. FTIR spectra of all other coumarin derivatives (ZL11-ZL16) is given in supplementary material (Figure S1-S18).

^{1}H NMR Study

Proton NMR spectroscopy is an important analytical method for determining the structure of substances associated with the hydrogen-1 nucleus in the molecule of the analyzed product. In the NMR spectra of all azo groups, peaks of aldehyde protons are observed at 9.5–10.3 ppm. The phenolic proton concentration of coumarin compounds is 11.0 to 1.5 ppm, but in these studies this value varies from 13 to 15 ppm for coumarin compounds [31]. ^{1}H NMR spectra of all synthesized compounds (ZL11-ZL16) were studied. All signals confirming the structure corresponding to the proton nucleus were evaluated by chemical shift values (ppm).). The experimental spectrum is almost identical to the theoretical spectrum obtained using chemsketch. ^{1}H NMR spectra allow us to identify the different chemical shifts of protons within a compound. The synthesis of compound ZL16 was confirmed through proton nuclear magnetic resonance (NMR) analysis, as illustrated in (Fig. 3). The spectrum revealed a sharp peak at 15.51 ppm, indicating the presence of exchangeable protons (OH). The analysis also identified multiple peaks at 7.82–7.80 ppm, corresponding to the proton (Hd, Ha) in the CH group. Another multiple peaks at 7.65–7.63 ppm were observed for protons (He, Hf) in the CH group, while doublet peak at 7.36 ppm indicated the presence of protons (Hb, Hc) in another CH group. Furthermore, singlet peak at 5.58 ppm were attributed to protons (Hg, Hh) in the CH group, and peaks at 2.49 ppm were associated with protons (Hi, Hj, Hk) in the CH group. This detailed analysis confirms the structural characteristics of compound ZL16 based on its proton NMR spectrum. ^{1}H NMR data of all other coumarin derivatives (ZL11-ZL16) is given in supplementary material (Figure S19-S24).

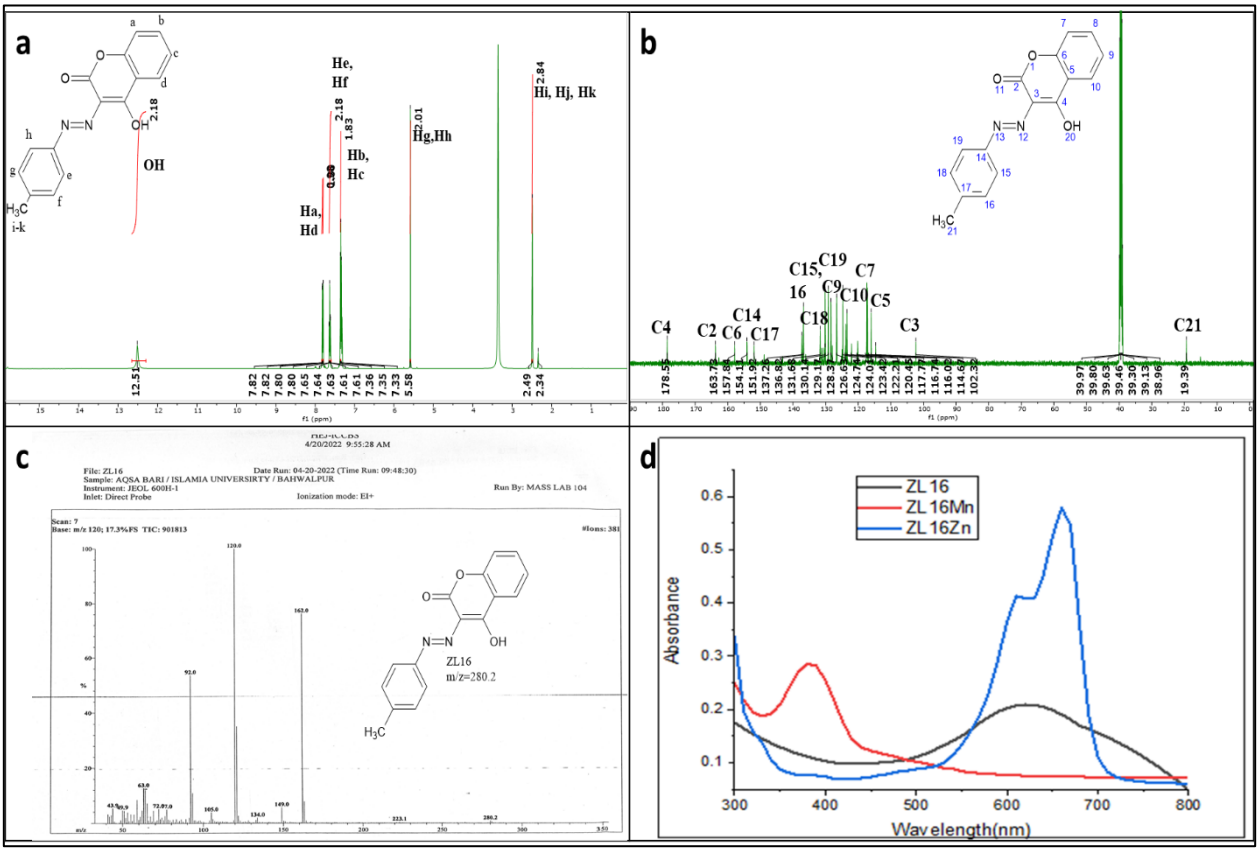

Figure 3. Spectra of (*a*) ^{1}H NMR of ZL16; (*b*) ^{13}C NMR of ZL16; (*c*) Mass spectrum of ZL16; (*d*) UV of ZL16

^{13}C NMR Study

The ^{13}C NMR spectra of compounds ZL11-ZL16 show a clear resonance in the direction of the carbon nucleus. NMR spectra of the new compounds were obtained on a Bruker AM400 MHz NMR spectrometer. All compounds were dissolved in DMSO-D6. The structures of all new compounds were confirmed by 1HNMR data. Direct signals of carbon for azo groups are detected at 136 and 152 ppm, and nitro, hydroxyl, and nitro groups are detected at 153, 125, and 142 ppm [85]. The confirmation of the synthesis of ZL16 derivative of coumarin compounds was established through the observation of distinct peaks in the 1HNMR spectrum. A sharp singlet peak was observed at a chemical shift at 178.5 ppm, indicating the presence of the C–OH (C4) group. The carbon atoms (C2, C6) attached to the nitrile group were evident in the region of 163.7 and 154.1 ppm. Peaks corresponding to the carbon atoms 151.9 (C14), 137.2 (C17), 130.1 (C15, C16), 129.1 (C19), 128.7 (C18), 124.7 (C9), 124.0 (C10), 117.7 (C7), 116.7 (C5), 102.3 (C3), 19.3 (C21) in the aromatic ring were observed. ^{13}C NMR data of all other coumarin derivatives (ZL11-ZL15) is given in supplementary material (Figure S25-S30).

UV-Visible Characterization of Synthesized Compounds

Coumarin derivatives ZL11–ZL16 and their metal complexes analyzed by UV-Visible spectroscopy and their spectra were recorded in DMSO solvent using 250 μL solution in the range of 200–800 nm. All the recorded UV-Vis spectra of coumarin derivatives ZL11–ZL16 and their metal complexes are illustrated in Figure S31–36 (Supporting file). The ultraviolet-visible (UV-Vis) spectra of the synthesized coumarin derivatives and their Mn(II) and Zn(II) complexes were recorded using 50 ppm solution of each compound in dimethyl sulfoxide (DMSO), and the measurements were conducted at room temperature within the wavelength range of 300–800 nm. The outcomes have been visually showed through comparative UV-Vis spectra, showed the λ_{max} peak in the range of 320–660. Interestingly, the synthesized coumarin derivatives exhibited significant absorbance in this region. In stark contrast, all the metal complexes demonstrated absorption maxima with weak absorbance peaks in the range of 380–670 nm. The Mn(II) complexes showcased intense absorption within the 390–660 nm region, whereas the Zn(II) complexes exhibited absorption within range 400–660 nm. These findings unequivocally indicate the successful synthesis of these metal complexes, as their absorption in the visible region strongly suggests their formation.

XRD Characterization of Synthesized Compounds

The XRD analysis of ligand ZL16 revealed distinct, sharp peaks at 2θ positions of 10.74°, 11.54°, 12.29°, 22.94°, and 29.26°, indicating a crystalline structure with an average crystal size of 4.092 nm. In contrast, the XRD pattern of its manganese complex (ZL16 Mn) showed the disappearance of these peaks and the emergence of new ones at 2θ positions of 17.27°, 26.69°, 31.54°, 34.75°, 38.69°, and 55.70°, with a slightly larger average crystal size of 4.34 nm, confirming the coordination of ZL16 with manganese. Similarly, the zinc complex exhibited peak shifts to 14.56°, 36.06°, 56.82°, 58.82°, and 61.30°, with an average crystal size of 1.574 nm, indicating successful complex formation with zinc. The sharpness of the peaks across all samples suggested their small size and crystalline nature, providing clear evidence of ligand coordination with both manganese and zinc metals. The crystallite sizes were calculated using the Scherer equation, ($D = 0.9\lambda/\beta \cos \theta$). The particle size of ligand ZL16, ZL16Mn and ZL16Zn complexes are found to be 4.092 nm, 4.341 nm and 1.574 nm respectively.

Thermo Analytical Results (TG and DTG) of Ligands and Metal Complex

The thermogravimetric analysis (TGA) of ZL14 reveals distinct decomposition stages across different metal variants. For ZL14, three decomposition stages occur between 45–500 °C: the first stage (45–150 °C) involves moisture and CO_2 evolution with a mass loss of 3.17 %; the second stage (150–350 °C) corresponds to the elimination of the azo group and Cl, resulting in a 20.39 % mass loss; the final stage (350–500 °C) leads to complete decomposition, leaving carbon as a residue with an 11.18 % mass loss. The total mass loss across these stages is 34.74 %, with an endothermic peak observed at 310 °C. In contrast, ZL14 Zn shows four decomposition stages from 32–500 °C: the first stage (32–150 °C) accounts for a 2.18 % mass loss due to water and CO_2; the second stage (150–200 °C) results in a 1.14 % mass loss from azo group elimination; the third stage (200–350 °C) involves the loss of heterocycles; and the final stage (350–450 °C) leads to carbon and ZnO formation with a 3.13 % mass loss. The total mass loss here is 9.59 %, with an endothermic peak at 180 °C. For ZL14 Mn, two decomposition stages are noted between 20–600 °C: the first stage (20–100 °C) results in an 8.76 % mass loss from moisture and CO_2, while the second stage (200–600 °C) corresponds to azo group elimination and yields an 8.77 % mass loss, culminating in carbon and MnO as final products. The total mass loss is 17.53 %, with an endothermic peak at 110 °C.

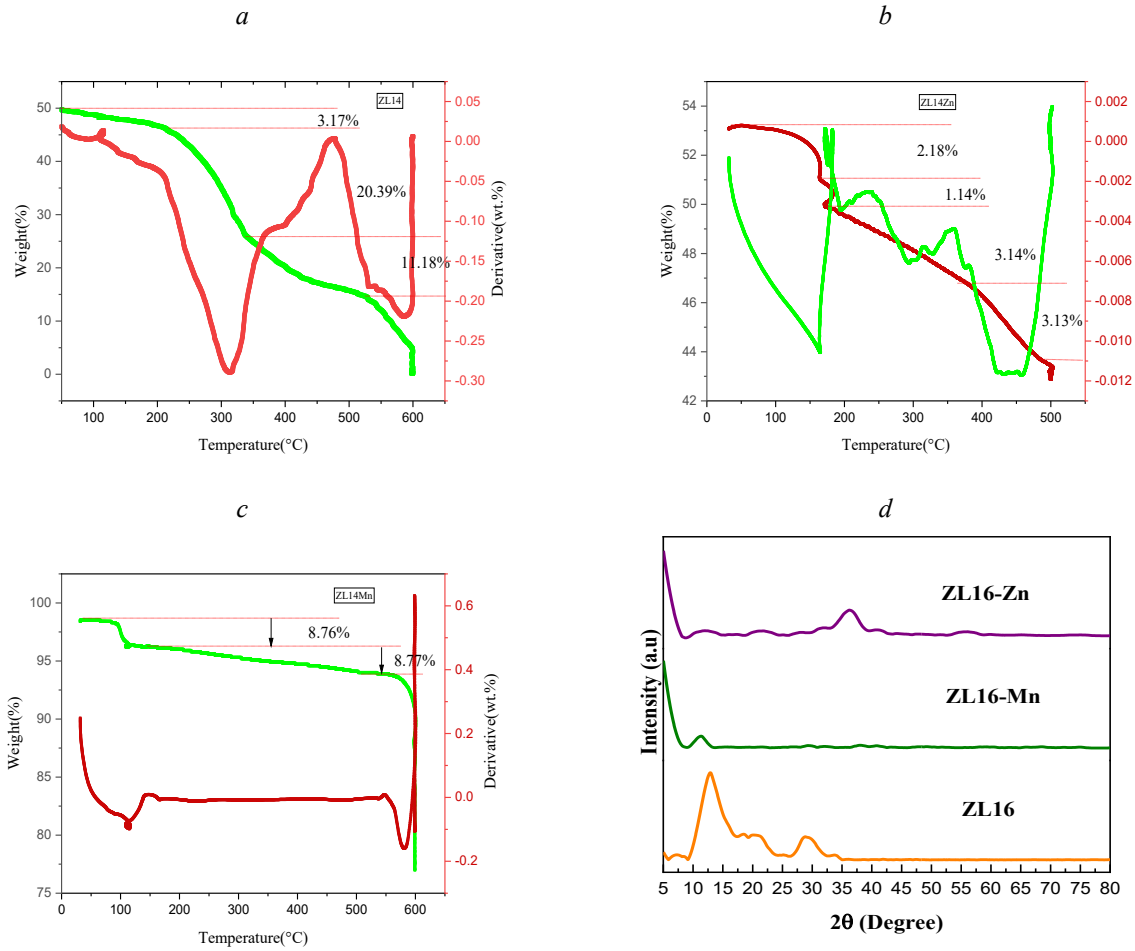

Figure 4. (*a*) TGA spectra of ZL14; (*b*) TGA spectra of ZL14Mn; (*c*) TGA spectra of ZL14Zn; (*d*) XRD of ZL16

Mass Spectrometric Study

Mass spectrometry is a method of determining the molecular mass of a substance [7]. Using this method, not only the peak information of the molecular ion but also information on the scattering pattern can be obtained, allowing the characteristics of the compound to be determined [8]. The quality of a compound can be determined using mass spectrometry methods. Information on molecular ion peaks, fragmentation patterns, and structural annotations were obtained through mass spectrometry. Therefore, in this study, we fixed the size of the coumarin ligand in the reaction model [4]. Mass spectra of synthesized compounds (ZL11–ZL16) are described in Figure S37–S42 (Supporting file). The molecular masses of the ZL11–ZL16 ligands are 282.25, 404.0, 280.8, 438.3, 300.1 and 280.2 which were confirmed in mass spectrometry studies, respectively. In the mass spectra of compound ZL16 (Fig. 5) the molecular ion peak appears at m/z value of 280.2 which is exact to the molecular mass of ZL16 (215.1) which is also the (most intense) base peak for this ligand. The possible modes of fragmentation for ZL16 ligand are given in Figure 5. Another important peak appeared at m/z value 119.1 by the removal of $C_9H_5O_3$ group from parent compound then the other important peak was seen at m/z value 91.0 by the removal of N_2 groups from 1st fragments (Route 1). The next important peak was appeared at m/z value 104.0 by the removal CH_3 from 1st fragment. Two peaks appeared at m/z value 76.0 and 49.9 from 2nd and 3rd fragment by the removal of N_2 and C_2H_2 respectively (Route 2). The next peaks were appeared at m/z value 120.0, 92.0 and 64.0 by the removal of $C_9H_8N_2O$, CO and CO radical from parent, 1st and 2nd fragment respectively (Route 3). The next important peak was appeared at m/z value 162.0 and 134.0 by the removal $C_7H_2O_2$ and CHO from parent and 1st fragment. Another important peak was seen at m/z 119.1 value by the removal of CH_3 group from 2nd fragment then other peak appeared at m/z value 93.0 by removal of N_2 from 3rd fragment. The peak of another important fragment was seen at m/z value 65.0 and 49.9 by the removal of N_2 and CH_3 radical from 4th and 5th fragment (Route 4).

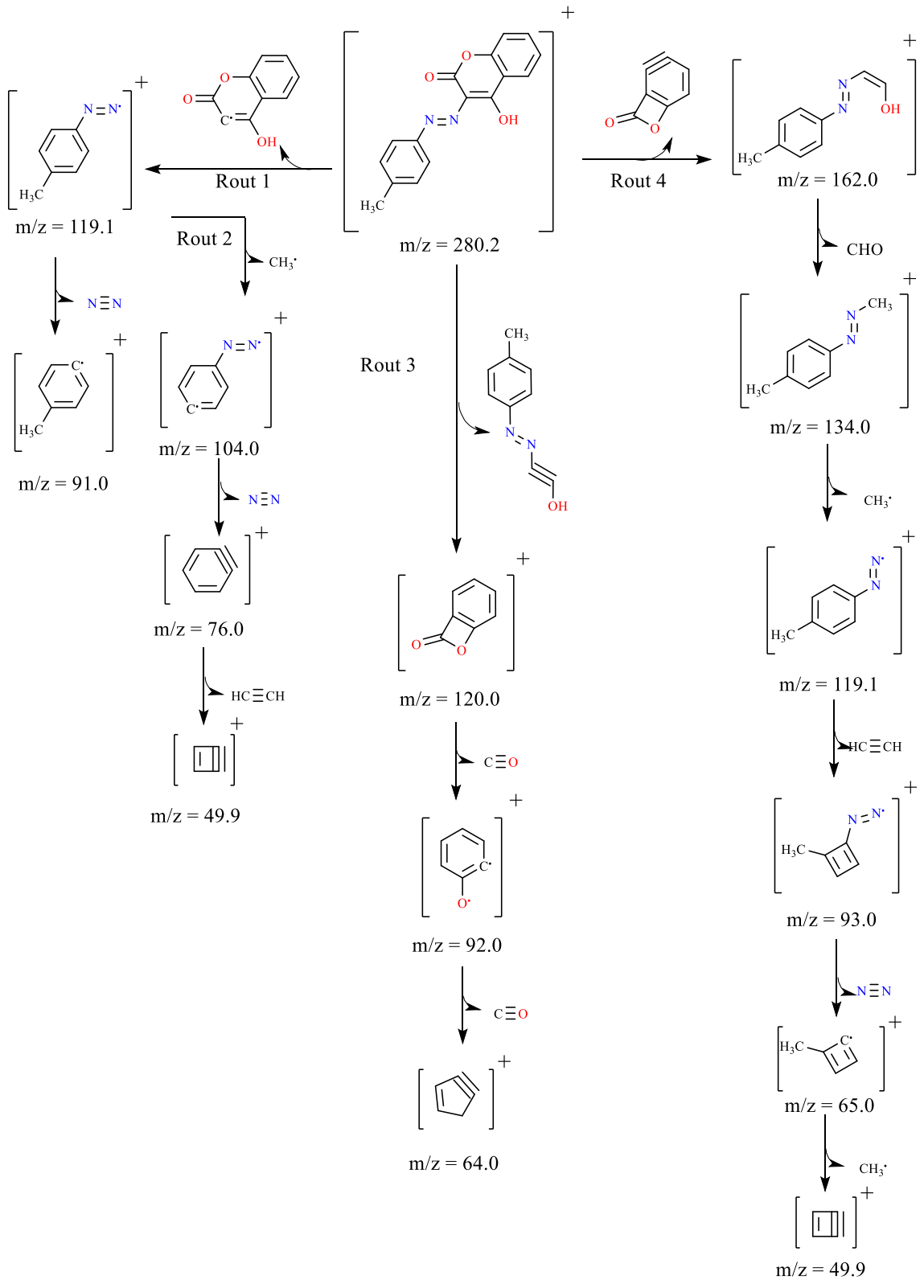

Figure 5. Mass spectrum fragmentation spectra ZL16

Free Radical Scavenging Potential of Coumarin Derivatives and Their Metal Complexes (ZL11-ZL16)

DPPH Radical Scavenging Assay

DPPH radical scavenging potential is a simple, efficient and relatively stable free radical method in which hydrogen or an electron is accepted by the reduction of free radical with the help of antioxidant mole-

cule. The solution of DPPH has purple color which is in reduced form changes to yellow. When more color change reduced more DPPH, radical enhance antioxidant activity. 579 nm absorbance is used for their calculation [32]. The DPPH radical scavenging activity of five concentrations (5, 10, 15, 20 and 25 μg/mL) of coumarin derivatives (ZL11–ZL16) and their manganese complexes (ZL11Mn–ZL16Mn) and zinc complexes (ZL11Zn–ZL16Zn) has been approved by ascorbic acid (AA) as standard. The results of antioxidant potential of prepared compounds are expressed in IC_{50} as given in Table 1.

Table 1

IC_{50} values of DPPH assay of coumarin derivatives and their metal complexes (ZL11–ZL16)

Compound	Scavenging of DPPH IC_{50}* (μg/mL)		
	ZL (Ligands)	Mn(II) Complex	Zn(II) Complex
ZL11	7.62±0.04	6.45±0.07	8.31±0.051
ZL12	6.93±0.05	11.84±0.01	6.10±0.048
ZL13	7.6±0.04	7.09±0.010	8.49±0.046
ZL14	7.78±0.03	11.04±0.01	5.65±0.080
ZL15	6.94±0.06	11.84±0.04	8.32±0.060
ZL16	6.57±0.03	6.62±0.02	7.14±0.075
AA**	7.066±0.06	7.066±0.06	7.066±0.06
Notes: * IC_{50} — is the concentration of compounds for 50 % inhibition of DPPH calculated by non-linear regression; ** AA — is the ascorbic acid (standard compound)			

All the prepared compounds display excellent inhibition potential as compared to standard (ascorbic acid) (7.06 μg/mL). Compounds ZL16, ZL11Mn and ZL14Zn, are more potent than that of ascorbic acid with IC_{50} = 6.57, 6.45 and 5.65 μg/m.

Nitric Oxide (NO) Radical Scavenging Assay

Nitric oxide (NO) is regarded as free radicals as they have unpaired electrons. NO is very reactive oxidant that can decompose to form OH and NO by the reaction with superoxide to form peroxinitrite anion. All the synthesized compounds displayed inhibition effect on nitrite ion generated from sodium nitroprusside in aqueous solution by reaction of oxygen with nitric oxide at biological pH. Griess reagent is used for calculating scavenging effect at decreased absorbance of 546 nm. All the prepared coumarin ligands and their metal complexes display better nitric oxide radical scavenging potential as compared to DPPH radical scavenging activity. The NO radical scavenging activity of five concentrations (5, 10, 15, 20 and 25 μg/mL) of coumarin derivatives (ZL11–ZL16) and their zinc complexes (ZL11Zn–ZL16Zn) has been approved by ascorbic acid (AA) (7.06 μg/mL) as standard. The results of antioxidant potential of prepared compounds are expressed in IC_{50} as given in Table 2.

Table 2

IC_{50} values of NO assays of coumarin derivatives and their metal complexes (ZL6-ZL10)

Compound	Scavenging of NO IC_{50}* (μg/mL)		
	ZL(Ligands)	Mn(II) (Complex)	Zn(II) (Complex)
ZL11	6.46±0.046	7.29±0.021	7.32±0.044
ZL12	6.38±0.095	5.99±0.060	6.77±0.078
ZL13	5.89±0.038	6.56±0.070	6.63±0.034
ZL14	7.015±0.068	6.98±0.024	6.07±0.09
ZL15	6.47±0.052	6.35±0.096	6.59±0.060
ZL16	11.2±0.053	7.10±0.670	6.30±0.065
AA**	6.79±0.026	6.79±0.026	6.79±0.026
Notes: * IC_{50} — is the concentration of compounds for 50 % inhibition of NO calculated by non-linear regression; ** AA — is the ascorbic acid (standard compound)			

All the prepared compounds display excellent inhibition potential as compared to standard (ascorbic acid). Compounds ZL12, ZL12Mn and ZL14Zn, are more potent than that of ascorbic acid with IC_{50} = 6.38, 5.99 and 6.07 μg/mL respectively.

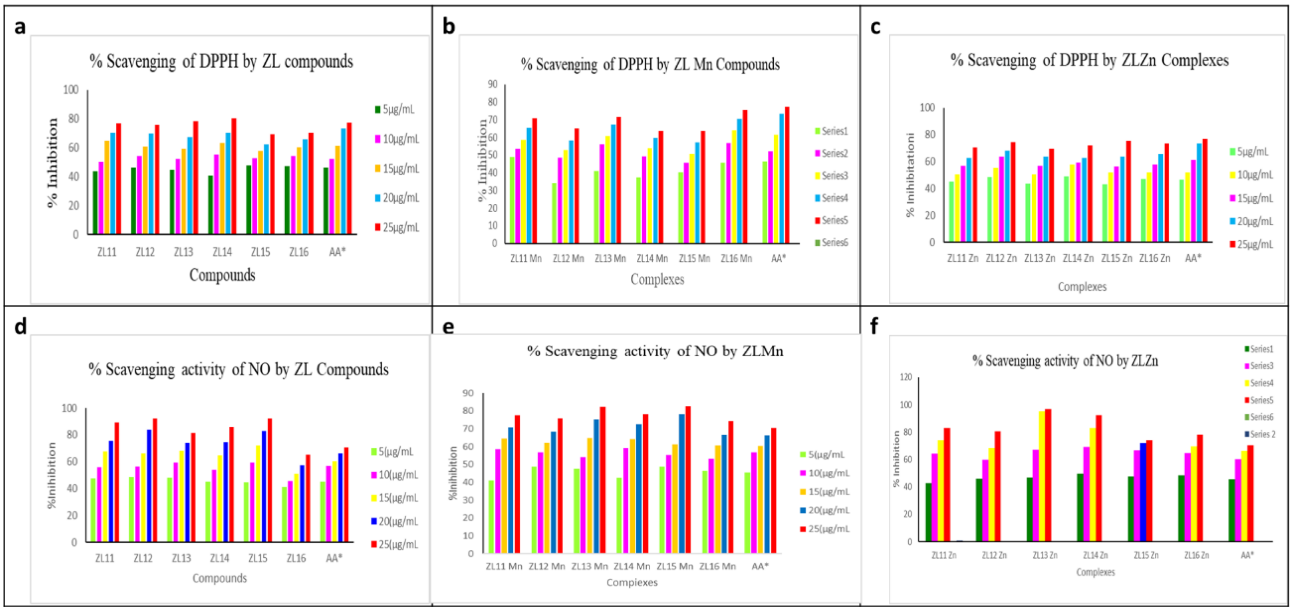

Figure 6. (*a*) Comparative graphical representation of DPPH scavenging activity by ZL compounds; (*b*) ZL Mn; (*c*) ZL Zn; (*d*) Comparative graphical representation of NO scavenging activity by ZL compounds; (*e*) ZL Mn; (*f*) ZL Zn

Antibacterial Activity

The in vitro antibacterial activity of coumarin compounds has been screened against *Staphylococcus Pyogenes* and *Bacillus* (gram positive bacteria) and *Escherichia Coli* and *Pseudomonas aeruginosa* (gram negative bacteria) by minimum inhibitory concentration (MIC). Amikacin was used as standard drug for the evaluation of antibacterial activity. Activity was reported by zone of inhibition (mm) [25]. The Zinc(II) complex have higher activity than other tested compounds due to the metal ions interaction with nitrogen. Biological screening results of Coumarin ligands shows that compound ZL13, ZL13Mn and ZL15Zn shown good antibacterial activity with zone of inhibition of 15 mm, 31 mm, and 28 mm respectively, against *E. Coli*, while all other compounds have zone of inhibition in the range 9–28 mm. The ligands ZL11, ZL16, ZL11Mn and ZL12Zn shown excellent activity with zone of inhibition of 18 mm, 18 mm, 18 mm and 23 mm respectively against Bacillus while all other compounds have zone of inhibition in the range 12–22 mm. Ligand ZL14, ZL12Mn and ZL16Zn shown good antibacterial activity with zone of inhibition of 15 mm,18 mm and 23 mm respectively, while all of other derivatives possessed activity against possessed activity against *Pseudomonas* while all other compounds have zone of inhibition in the range 9–22 mm. Ligand ZL12, ZL12Mn and ZL11Zn shown activity against *Staphylococcus Pyogenes* with zone of inhibition of 16 mm, 20 mm and 20 mm respectively while all other compounds have zone of inhibition in the range 9–16 mm. Zone of inhibition for standard drug Amikacin is 15 mm. The biological screening of Coumarin ligands revealed promising findings. Against *Escherichia Coli,* compound ZL16 demonstrated good antibacterial activity, resulting in a zone of inhibition of 16 mm as shown in Table 3–5.

Table 3

Antibacterial activity of coumarin derivatives ZL11-ZL16

Compound	Zone of Inhibition (mm)			
	Gram-negative bacteria		Gram-positive bacteria	
	E. coli	*Pseudomonas*	*S. Pyogenes*	*Bacillus*
ZL11	9	12	15	18
ZL12	11	8	16	18
ZL13	15	12	9	14
ZL14	12	15	10	16
ZL15	13	8	14	17
ZL16	14	22	16	18
Amikacin	15	13	16	15

Table 4

Antibacterial activity of metal complexes ZL11Mn-ZL16Mn

Compound No.	Zone of Inhibition (mm)			
	Gram-negative bacteria		Gram-positive bacteria	
	E. coli	*Pseudomonas*	*S. Pyogenes*	*Bacillus*
ZL11Mn	18	14	13	18
ZL12 Mn	20	18	20	10
ZL13 Mn	31	10	8	12
ZL14 Mn	8	8	9	14
ZL15 Mn	11	11	9	16
ZL16 Mn	12	9	7	18
Amikacin	14	16	15	13

Table 5

Antibacterial activity of metal complexes ZL11Zn-ZL16Zn

Compound No.	Zone of Inhibition (mm)			
	Gram-negative bacteria		Gram-positive bacteria	
	E. coli	*Pseudomonas*	*S. Pyogenes*	*Bacillus*
ZL11 Zn	12	9	20	20
ZL12 Zn	14	15	15	23
ZL13 Zn	12	11	14	21
ZL14 Zn	13	12	16	18
ZL15 Zn	28	13	15	17
ZL16 Zn	22	23	13	22
Amikacin	16	14	16	14

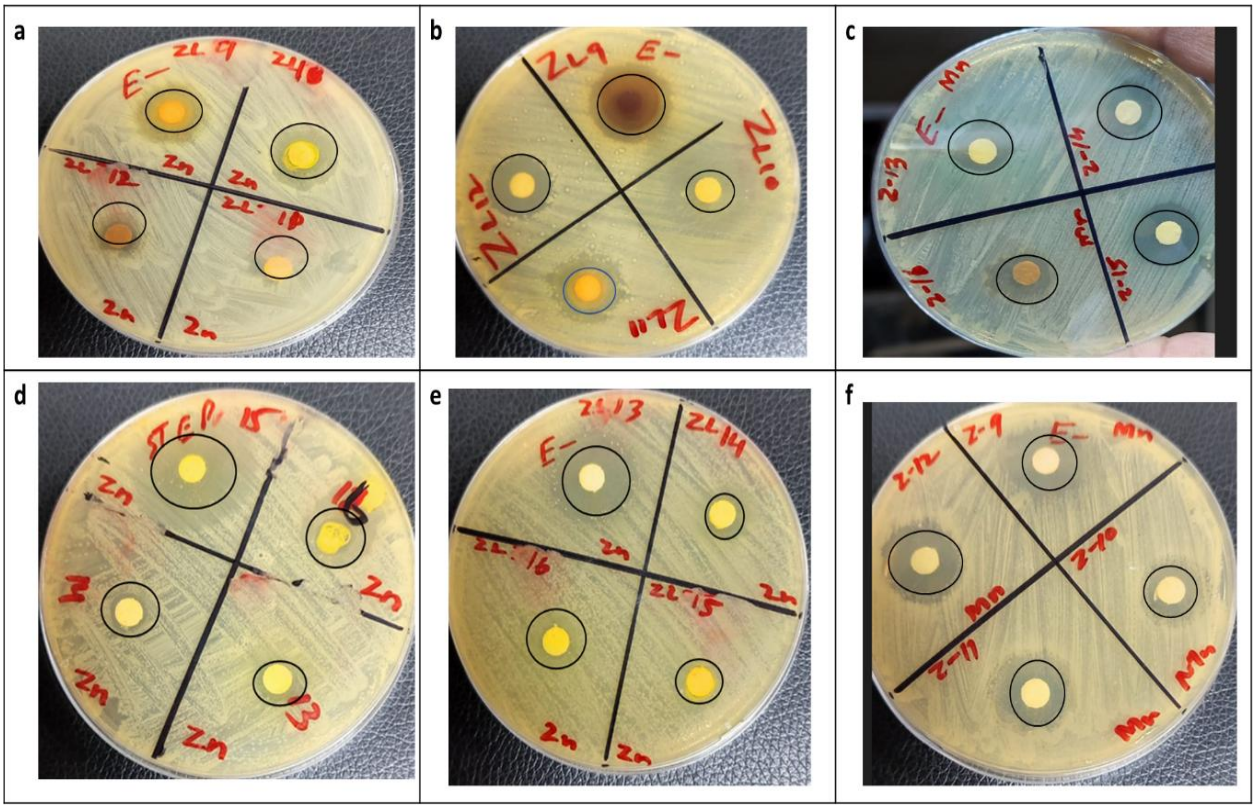

Figure 7. Anti-Bacterial activities of coumarin derivatives and their metal complexes (ZL11–ZL16)

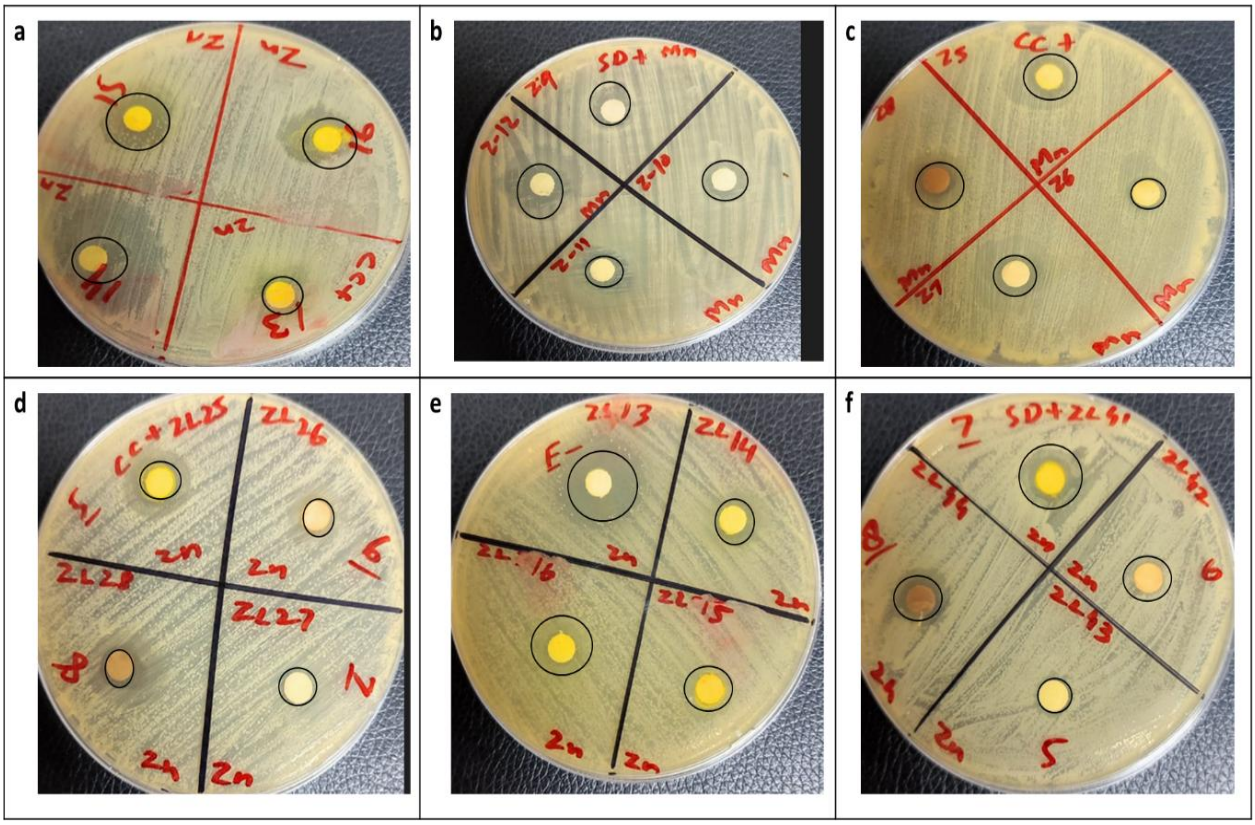

Figure 8. Anti-Bacterial activities of coumarin derivatives and their metal complexes (ZL11–ZL16)

Molecular Docking Analysis

In order to understand the mechanism of action, the molecular interaction between the synthesized ligands and two specific enzymes, Oligo-1,6-glucosidase (PDB ID: 3AJ7) and Mannosyl-oligosaccharide glucosidase (PDB ID: 4J5T), was studied. The resolution of the Oligo-1,6-glucosidase structure was 1.30Å, while the resolution of the Mannosyl-oligosaccharide glucosidase structure was 2.04Å. The results of the study revealed that hydrogen bonds were formed when a hydrogen atom interacted with an electronegative atom, such as oxygen or nitrogen. To investigate the binding interactions between the ligands (ZL11–ZL16) and their metal complexes with the binding pocket of Mannosyl-oligosaccharide and Oligo-1,6-glucosidase, molecular docking analysis was conducted. The docking analysis yielded highly convincing results, indicating strong binding interactions between several amino acid residues within the binding pocket of Mannosyl-oligosaccharide glucosidase and Oligo-1,6-glucosidase. These findings provide valuable insights into potential lead compounds for drug development targeting mannosyl-oligosaccharide glucosidase and Oligo-1,6-glucosidase. The docking analysis of Oligo-1,6-glucosidase also produced convincing results, indicating strong interactions between several amino acid residues within its binding pocket and the ZL16, ZL16Mn, and ZL16Zn compounds as shown in Figure 9. The binding energies for these interactions were determined to be –9.8, –10.9 and –10.8 kcal/mol, respectively as given in Table 6.

Similarly, the docking analysis yielded highly convincing results, indicating strong binding interactions between several amino acid residues within the binding pocket of Mannosyl-oligosaccharide glucosidase and the ZL15, ZL15Mn, and ZL15Zn compounds as shown in Figure 8. The binding energies for these interactions were determined to be –10.1, –10.3, and –10.6 kcal/mol, respectively as given in Table 7. These findings suggest that the synthesized ligands have the potential to interact strongly with the binding pockets of both Mannosyl-oligosaccharide glucosidase and Oligo-1,6-glucosidase.

Table 6

Molecular Docking of compounds (ZL11-ZL16) with Oligo-1,6-glucosidase and mannosyl-oligosaccharide glucosidase

Ligand Codes	PDB ID	Binding energy, kcal/mol	Hydrogen bonds interactions	Hydrophobic interactions
ZL11	3AJ7	–8.6	LYS156	LEU313, ALA418, PHE314, ILE419, ASP233
	4J5T	–9.0	HIS803, ARG799, ASP724	GLU463, GLU402, ARG727, MET401
ZL12	3AJ7	–8.6	No	LYS156, TYR158, PHE303
	4J5T	–9.7	ARG428	ASP392, GLU771, ASP568, TYR709, LEU563, PHE444
ZL13	3AJ7	–8.7	HIS295, ASN259, ILE272	VAL266, ALA292, ARG263
	4J5T	–9.4	HIS803, ARG799, ASP724	ARG727, ARG467
ZL14	3AJ7	–10.1	No	LYS156, TYR158, PHE303
	4J5T	–8.3	ARG428	GLU771, ASP392, ASP568, TYR709, LEU563, PHE444
ZL15	3AJ7	–10.1	HIS295, ASN259, ILE272	VAL266, ALA292, ARG263
	4J5T	–9.3	HIS803, ARG799, ASP724	ARG727, ARG467
ZL16	3AJ7	–8.8	ASN317, LYS156	LEU313, ASP233, ALA418, PHE314, ILE419
	4J5T	–9.8	NO	ARG727, GLU402, GLU463, SER802, MET401, PRO731, ILE734

Table 7

Molecular Docking metal complexes (ZL11-ZL16) with Oligo-1,6-glucosidase and mannosyl-oligosaccharide glucosidase

Ligand Codes	PDB ID	Binding energy, kcal/mol	Hydrogen bonds interactions	Hydrophobic interactions
ZL11Mn	3AJ7	–9.1	PHE321	LEU439
	4J5T	–9.8	TYR709	PHE444, PHE389, PHE385, PRO441
ZL11Zn	3AJ7	–9.7	PHE543, LEU323, LYS523	PHE321
	4J5T	–8.9	MET493, ARG304	PHE7, LYS98
ZL12Mn	3AJ7	–8.1	NO	GLU332, ALA329, ILE328, PRO312, HIS280
	4J5T	–8.6	LYS597, LYS669	HIS601, TYR728, GLU616
ZL12Zn	3AJ7	–9.4	ASP363	PHE321, LEU439, ASP362
	4J5T	–8.9	HIS561.ARG428	PHE444, PRO441, PHE385, TYR709, LEU563
ZL13Mn	3AJ7	–9.1	PHE321	LEU439
	4J5T	–9.5	ARG387	PHE444, ALA783, PHE385, PHE384
ZL13Zn	3AJ7	–9.1	NO	
	4J5T	–10.2	HIS561	LEU563, ARG428, GLU707
ZL14Mn	3AJ7	–8.7	SER545	ASP362, LEU439, LYS524
	4J5T	–10.4	TYR709, ARG387	GLU771, PHE444
ZL14Zn	3AJ7	–10.2	NO	
	4J5T	–9.6	NO	TYR709, PHE385, PHE444, PRO441
ZL15Mn	3AJ7	–10.3	NO	PRO312
	4J5T	–12.2	NO	PHE444, ILE362, ILE451, LYS363
ZL15Zn	3AJ7	–10.6	LYS523, LEU323	LEU439
	4J5T	–12.7	ASP568, TRP710	ARG428, TYR709, PHE385
ZL16Mn	3AJ7	–8.9	NO	LYS523, PHE360, LEU323, LEU439
	4J5T	–10.9	NO	LYS98, PHE7, ARG304, GLU10, LYS6
ZL16Zn	3AJ7	–9.1	ASP363	LEU439, PHE321
	4J5T	–10.8	HIS561, ARG428	TRP710, LEU563, PHE389, PHE385, GLU707

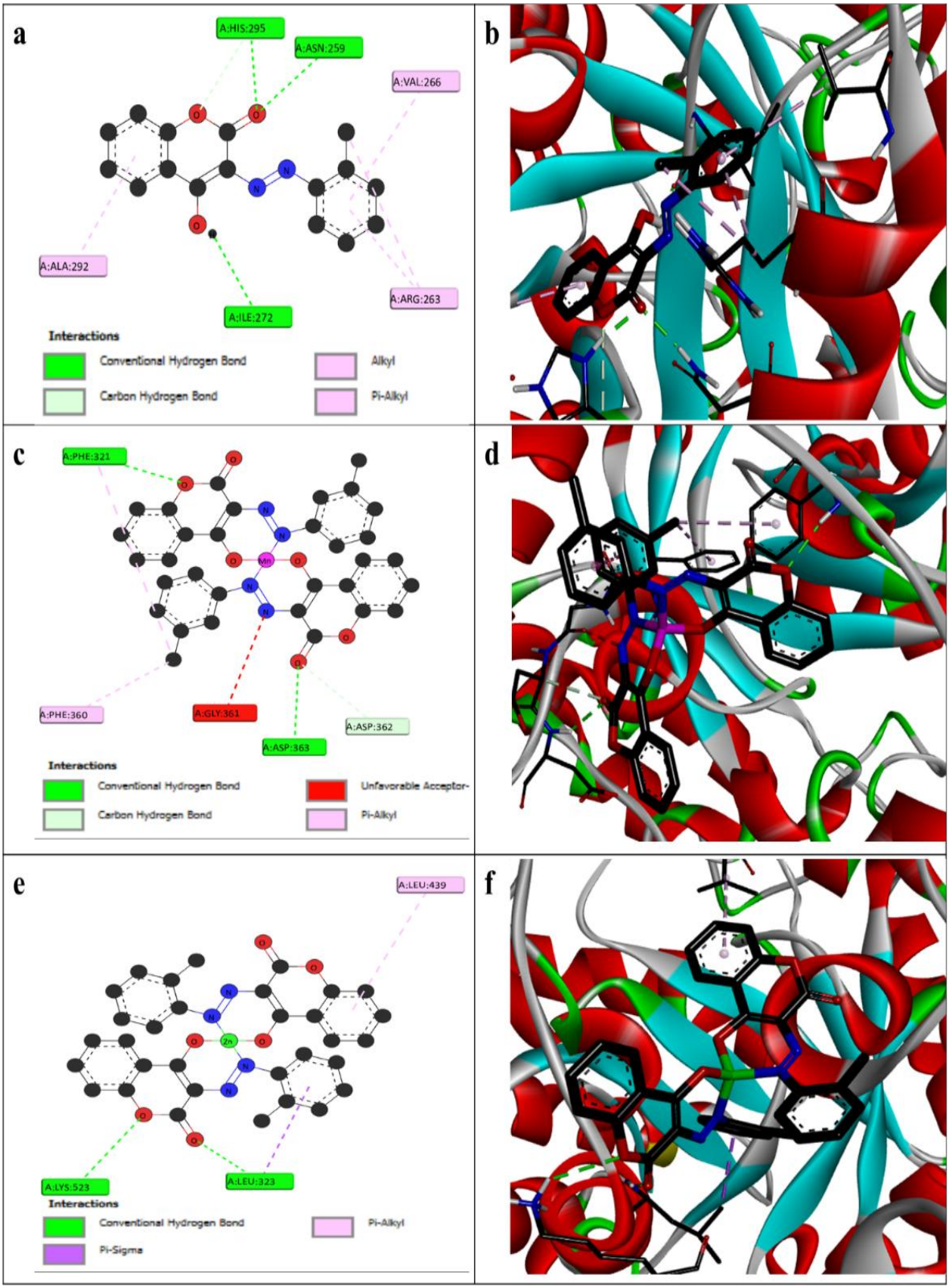

Figure 9. (*a*) Most probable 2D and (*b*) 3D binding modes of ZL15; (*c*) 2D ZL15Mn; (*d*) 3D ZL15Mn; (*e*) 2D ZL15Zn; (*f*) 3D ZL15Zn

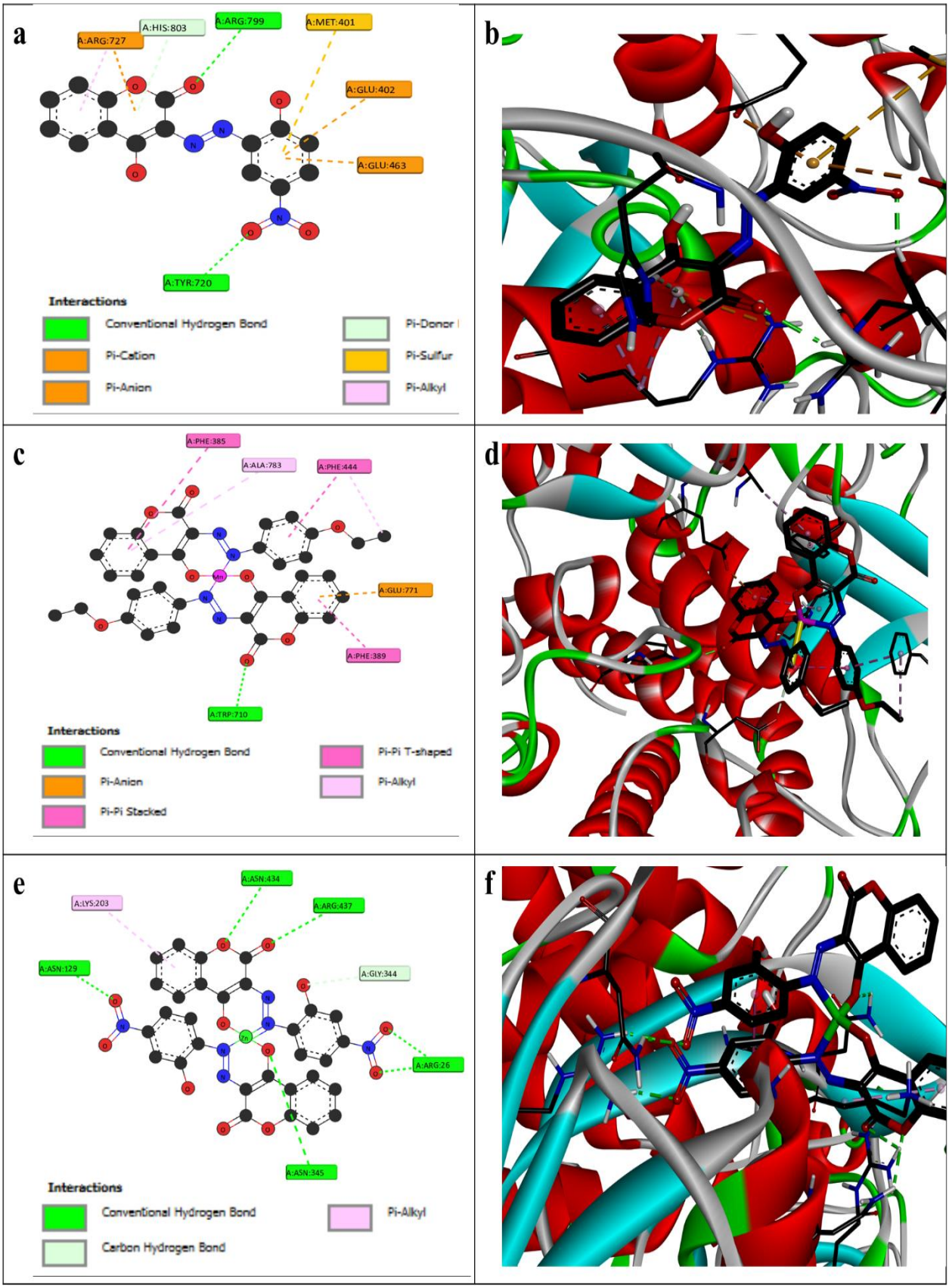

Figure 10. (*a*) Most probable 2D and (*b*) 3D binding modes of ZL16; (*c*) 2D ZL16Mn; (*d*) 3D ZL16Mn; (*e*) 2D ZL16Zn; (*f*) 3D ZL16Zn

Conclusions

In a recent study, researchers successfully synthesized several new medicinal coumarin derivatives using a synthesis process that is both environmentally friendly and efficient. The compounds synthesized include 4-hydroxycoumarin, 2-aminophenol, 2-amino-5-chlorobenzophenone, o-toluidine, 2'-amino-2,5-dichlorophenylphenone, 2-chloroaniline, p-toluidine. The synthesis process achieved excellent yields ranging from 70 % to 87 % at temperatures between 0–5 °C. To determine the structure of the synthesized compounds, various characterization methods were employed, including FTIR, ^{1}H NMR, ^{13}C NMR, UV/VIS, XRD, and TGA. Mass spectroscopy was also used to confirm the mass of the synthesized compounds. The FTIR spectra analysis revealed the presence of functional groups such as O–H stretch, N–H stretch, and N=N group, which confirmed the successful synthesis of the ligands. The spectra also showed peaks corresponding to sp^3 CH_3 stretch, aromatic C–H stretch, carbonyl group C–O stretch, C=C stretch, and aromatic C–N stretch. Interestingly, the phenolic proton concentration of most coumarin compounds typically falls within the range of 11.0 to 1.5 ppm. However, in this study, the values varied from 13 to 15 ppm for the coumarin compounds, indicating some structural differences. The ^{13}C NMR analysis of the coumarin derivatives revealed specific peaks corresponding to the 6 signals of carbon for azo- groups and nitro-, hydroxyl-, and nitro- groups were also detected. To further characterize the synthesized compounds and their metal complexes, UV-Visible analysis was conducted in the 300–600 nm range, and powder XRD analysis was performed. The XRD results indicated crystal sizes for ZL16, ZL16Mn, and ZL16Zn as 4.092 nm, 4.341 nm, and 1.574 nm, respectively. Thermal stability was assessed through TGA analysis, which demonstrated that the synthesized compounds exhibited thermal stability up to 800 °C. The synthesized ligands and their metal complexes were then subjected to screening for antibacterial, molecular docking, and antioxidant activities.

Antibacterial activity was assessed against gram-negative bacteria (E. coli and Pseudomonas) and gram-positive bacteria (Staphylococcus pyogenes and Bacillus), with inhibition zones ranging from 7–31 mm, while Amikacin showed a zone of inhibition of 15 mm. In terms of DPPH antioxidant activity, compounds ZL16, ZL11Mn, and ZL14Zn demonstrate greater potency than ascorbic acid, with IC_{50} values 6.57, 6.45 and 5.65 µg/mL respectively. In same way DPPH antioxidant activity, compounds ZL12, ZL12Mn, and ZL14Zn demonstrate greater potency than ascorbic acid, with IC_{50} values 6.38, 5.99 and 6.07 µg/mL respectively. The docking analysis revealed strong binding interactions between the Mannosyl-oligosaccharide glucosidase binding pocket and ZL15, ZL15Mn, and ZL15Zn compounds, with binding energies of –10.1, –10.3, and –10.6 kcal/mol, respectively. Similarly, Oligo-1,6-glucosidase showed strong interactions with the ZL16, ZL16Mn, and ZL16Zn compounds, with binding energies of –9.8, –10.9, and –10.8 kcal/mol, respectively. In conclusion, this study successfully synthesized new medicinal coumarin derivatives and their metal complexes using an environmentally friendly synthesis process. The compounds exhibited significant antibacterial and antioxidant activities, as well as promising results in molecular docking studies. These findings contribute to the field of medicinal chemistry and hold promise for the development of potential therapeutic agents. Further investigations are warranted to explore their full potential.

Supporting Information

The Supporting Information is available free at https://ejc.buketov.edu.kz/ejc/article/view/479/322

*Author Information**

**The authors' names are presented in the following order: First Name, Middle Name and Last Name*

Zulfiqar Ali Shahid — PhD Scholar; Institute of Chemistry, Islamia University of Bahawalpur, 63100, Bahawalpur, Pakistan e-mail: zulfiqar.ali.shahid1980@gmail.com; https://orcid.org/0009-0004-0722-7563

Rukhsana Tabassum (*corresponding author*) — Assistant Professor; Institute of Chemistry, Islamia University of Bahawalpur, 63100, Bahawalpur, Pakistan; e-mail: rukhsana.tabassum@iub.edu.pk; https://orcid.org/0000-0002-9483-254X

Author Contributions

The manuscript was written through contributions of all authors. All authors have given approval to the final version of the manuscript. CRediT: **Zulfiqar Ali Shahid** — investigation, validation, formal analysis, — writing-original draft, writing-review & editing; **Rukhsana Tabassum** — design, conceptualization, methodology, supervision.

Acknowledgments

Authors are grateful to the Institute of Chemistry-IUB for providing essential facilities. Authors also acknowledge the Higher Education Commission for providing analyses facility via ASIP.

Declaration of Generative AI and AI-Assisted Technologies in the Writing Process

During the preparation of this work the authors used Grammarly in order to refine the language of the manuscript. After using this service, the authors reviewed and edited the content as needed and take full responsibility for the content of the publication.

Conflicts of Interest

The authors declare no conflict of interest.

References

1 Abdel-Latif, S. A., & Moustafa, H. (2018). Synthesis, spectroscopic properties, density functional theory calculations, and nonlinear optical properties of novel complexes of 5-hydroxy-4,7-dimethyl-6-(phenylazo) coumarin with Mn(II), Co(II), Ni(II), Cu(II), and Zn(II) metal ions. *Applied Organometallic Chemistry, 32*(4), e4269. https://doi.org/10.1002/aoc.4269

2 Adimule, V. M., Nandi, S. S., Kerur, S., Khadapure, S. A., & Chinnam, S. (2022). Recent advances in the one-pot synthesis of coumarin derivatives from different starting materials using nanoparticles: A review. *Topics in Catalysis*, 1-31. https://doi.org/10.1007/s11244-022-01554-0

3 Anderson, N. C., Hendricks, M. P., Choi, J. J., & Owen, J. S. (2013). Ligand exchange and the stoichiometry of metal chalcogenide nanocrystals: Spectroscopic observation of facile metal-carboxylate displacement and binding. *Journal of the American Chemical Society, 135*(49), 18536–18548. https://doi.org/10.1021/ja4091298

4 Attaullah, H. M., Ejaz, S. A., Channar, P. A., Saeed, A., Ujan, R., Zargar, S., Channar, S. A., Sahito, R., Wani, T. A., & Abbas, Q. (2024). Exploration of newly synthesized azo-thiohydantoins as potential alkaline phosphatase inhibitors via advanced biochemical characterization and molecular modeling approaches. *BMC Chemistry, 18*(1), 47. https://doi.org/10.1186/s13065-024-00472-3

5 Balewski, Ł., Szulta, S., Jalińska, A., & Kornicka, A. (2021). A mini-review: Recent advances in coumarin-metal complexes with biological properties. *Frontiers in Chemistry*, 9, 781779. https://doi.org/10.3389/fchem.2021.781779

6 Bazargani, M. M., & Rohloff, J. (2016). Antibiofilm activity of essential oils and plant extracts against Staphylococcus aureus and Escherichia coli biofilms. *Food Control*, 61, 156–164. https://doi.org/10.1016/j.foodcont.2015.09.036

7 Catapano, M. C., Karlíčková, J., Tvrdý, V., Sharma, S., Prasad, A. K., Saso, L., Chhillar, A. K., Kuneš, J., Pour, M., & Parmar, V. S. (2018). Mono and dihydroxy coumarin derivatives: Copper chelation and reduction ability. *Journal of Trace Elements in Medicine and Biology*, 46, 88–95. https://doi.org/10.1016/j.jtemb.2017.10.003

8 Filipsky, T., Riha, M., Macakova, K., Anzenbacherová, E., Karlickova, J., & Mladenka, P. (2015). Antioxidant effects of coumarins include direct radical scavenging, metal chelation, and inhibition of ROS-producing enzymes. *Current Topics in Medicinal Chemistry, 15*(5), 415–431. https://doi.org/10.2174/1568026614666150407124745

9 Garg, S. S., Gupta, J., Sharma, S., & Sahu, D. (2020). An insight into the therapeutic applications of coumarin compounds and their mechanisms of action. *European Journal of Pharmaceutical Sciences*, 152, 105424. https://doi.org/10.1016/j.ejps.2020.105424

10 Ghanghas, P., Choudhary, A., Kumar, D., & Poonia, K. (2021). Coordination metal complexes with Schiff bases: Useful pharmacophores with comprehensive biological applications. *Inorganic Chemistry Communications*, 130, 108710. https://doi.org/10.1016/j.inoche.2021.108710

11 Gupta, A., Mumtaz, S., Li, C.-H., Hussain, I., & Rotello, V. M. (2019). Combatting antibiotic-resistant bacteria using nanomaterials. *Chemical Society Reviews, 48*(2), 415–427. https://doi.org/10.1039/C7CS00857J

12 Houas, N., Chafaa, S., Chafai, N., Ghedjati, S., Djenane, M., & Kitouni, S. (2022). Synthesis, characterization, DFT study, and antioxidant activity of (2-hydroxynaphthalen-1-yl)methyl-2-hydroxyphenylamino phosphonic acid. *Journal of Molecular Structure*, 1247, 131322. https://doi.org/10.1016/j.molstruc.2021.131322

13 Kadhum, A. A. H., Al-Amiery, A. A., Musa, A. Y., & Mohamad, A. B. (2011). The antioxidant activity of new coumarin derivatives. *International Journal of Molecular Sciences, 12*(9), 5747–5761. https://doi.org/10.3390/ijms12095747

14 Kapur, A., Hasković, A., Čopra-Janićijević, A., Klepo, L., Topčagić, A., Tahirović, I., & Sofić, E. (2012). Spectrophotometric analysis of total ascorbic acid content in various fruits and vegetables. *Bulletin of the Chemists and Technologists of Bosnia and Herzegovina, 38*(4), 39–42. https://doi.org/10.35773/bctbh.2012.38.4.39

15 Kaur, H., Lim, S. M., Ramasamy, K., Vasudevan, M., Shah, S. A. A., & Narasimhan, B. (2020). Diazenyl Schiff bases: Synthesis, spectral analysis, antimicrobial studies, and cytotoxic activity on human colorectal carcinoma cell line (HCT-116). *Arabian Journal of Chemistry, 13*(1), 377–392. https://doi.org/10.1016/j.arabjc.2016.08.004

16 Keri, R. S., Sasidhar, B., Nagaraja, B. M., & Santos, M. A. (2015). Recent progress in the drug development of coumarin derivatives as potent antituberculosis agents. *European Journal of Medicinal Chemistry*, 100, 257–269. https://doi.org/10.1016/j.ejmech.2015.06.037

17 Kharadi, G. (2012). Thermal decomposition and mass spectra of mixed ligand copper (II) complexes of 1,10-phenanthroline and coumarin derivatives. *Journal of Thermal Analysis and Calorimetry, 107*(2), 651–659. https://doi.org/10.1007/s10973-011-1760-2

18 Lončarić, M., Gašo-Sokač, D., Jokić, S., & Molnar, M. (2020). Recent advances in the synthesis of coumarin derivatives from different starting materials. *Biomolecules, 10*(1), 151. https://doi.org/10.3390/biom10010151

19 Maobe, M. A., & Nyarango, R. M. (2013). Fourier transformer infra-red spectrophotometer analysis of Urtica dioica medicinal herb used for the treatment of diabetes, malaria, and pneumonia in Kisii region, Southwest Kenya. *World Applied Sciences Journal, 21*(8), 1128–1135. https://doi.org/10.5829/idosi.wasj.2013.21.8.1898

20 Marchi, R. C., Campos, I. A., Santana, V. T., & Carlos, R. M. (2022). Chemical implications and considerations on techniques used to assess the in vitro antioxidant activity of coordination compounds. *Coordination Chemistry Reviews*, 451, 214275. https://doi.org/10.1016/j.ccr.2022.214275

21 Ndagi, U., Mhlongo, N., & Soliman, M. E. (2017). Metal complexes in cancer therapy–an update from a drug design perspective. *Drug Design, Development and Therapy*, 599–616. https://doi.org/10.2147/DDDT.S134156

22 Olson, E. J., & Bülmann, P. (2011). Getting more out of a Job plot: Determination of reactant to product stoichiometry in cases of displacement reactions and n:n complex formation. *The Journal of Organic Chemistry, 76*(20), 8406–8412. https://doi.org/10.1021/jo2015719

23 Patil, S. A., Unki, S. N., & Badami, P. S. (2013). Synthesis, characterization, biological and thermal behavior of Co(II), Ni(II), and Cu(II) complexes with Schiff bases having coumarin moieties. *Journal of Thermal Analysis and Calorimetry*, 111, 1281–1289. https://doi.org/10.1007/s10973-012-2809-2

24 Peng, X.-M., LV Damu, G., & Zhou, H. (2013). Current developments of coumarin compounds in medicinal chemistry. *Current Pharmaceutical Design, 19*(21), 3884–3930. https://doi.org/10.2174/1381612811319210010

25 Retnam, C. G., Rose, S. V., & Kumari, B. S. (2023). Synthesis, characterization, biological activity, and molecular docking study of transition metal complexes from heterocyclic ligand system. *Journal of Molecular Structure*, 1282, 135162. https://doi.org/10.1016/j.molstruc.2023.135162

26 Sharma, T., Singh, D., Mahapatra, A., Mohapatra, P., Sahoo, S., & Sahoo, S. K. (2022). Advancements in clinical translation of flavonoid nanoparticles for cancer treatment. *OpenNano*, 100074. https://doi.org/10.1016/j.opnano.2022.100074

27 Sohrabi, M., Binaeizadeh, M. R., Iraji, A., Larijani, B., Saeedi, M., & Mahdavi, M. (2022). A review on α-glucosidase inhibitory activity of first-row transition metal complexes: A futuristic strategy for the treatment of type 2 diabetes. RSC Advances, 12(19), 12011–12052. https://doi.org/10.1039/D2RA02383A

28 Souhangir, M., Bidoki, S. M., & Gharanjig, K. (2022). Synthesis of a novel fluorescent reactive dye based on coumarin-benzimidazole for high visibility dyeing of cotton. *Progress in Color, Colorants and Coatings, 15*(4), 327–340. https://doi.org/10.1515/pccc-2022-0024

29 Sunitha, N., Raj, C. I. S., & Kumari, B. S. (2023). Synthesis, spectral studies, biological evaluation, and molecular docking studies of metal complexes from coumarin derivative. *Journal of Molecular Structure*, 1285, 135443. https://doi.org/10.1016/j.molstruc.2023.135443

30 Wiester, M. J., Ulmann, P. A., & Mirkin, C. A. (2011). Enzyme mimics based upon supramolecular coordination chemistry. Angewandte Chemie International Edition, 50(1), 114–137. https://doi.org/10.1002/anie.201004563

31 Zaidan, M., Noor Rain, A., Badrul, A., Adlin, A., Norazah, A., & Zakiah, I. (2005). In vitro screening of five local medicinal plants for antibacterial activity using disc diffusion method. *Trop Biomed, 22*(2), 165–170.

32 Zhang, G., Zheng, H., Guo, M., Du, L., Liu, G., & Wang, P. (2016). Synthesis of polymeric fluorescent brightener based on coumarin and its performances on paper as light stabilizer, fluorescent brightener, and surface sizing agent. *Applied Surface Science*, 367, 167–173. https://doi.org/10.1016/j.apsusc.2016.01.031